A Method of State Estimation for Underwater Vehicle Navigation Around A Cylindrical Structure

Teng Zhang, Shoudong Huang, Dikai Liu, Lei Shi
Centre for Autonomous Systems, University of Technology, Sydney, Australia
{Teng.Zhang, Shoudong.Huang, Dikai.Liu, Lei.Shi-1}@uts.edu.au
Chunlin Zhou, Rong Xiong
Institute of Cyber-Systems and Control, Zhejiang University, China
c_zhou@zju.edu.cn, rxiong@iipc.zju.edu.cn

***Abstract*—Recently, increasing efforts have been focused on the development and adoption of autonomous underwater vehicles (AUVs) for various applications. However, the GPS signals are usually unavailable, the vehicle dynamics is very uncertain, and the complicated vision based localization algorithms may not work well in the underwater environments. Hence, accurate and timely state estimation using low-cost sensors remains a challenge for the control and navigation of AUVs. This paper considers the state estimation problem for underwater vehicle navigation around a cylindrical structure. The vehicle is assumed to be equipped with only low-cost sensors: an inertia measurement unit (IMU), a pressure sensor and a monocular camera. By exploiting the prior knowledge on the size and shape of the structure, an efficient algorithm for estimating the state of the AUV is developed without using any dynamic model. Firstly, a state observer is proposed under the condition that the localization result (rotational and translational position) is available. Next, we present a method for localization based on the IMU readings, pressure sensor readings and the image of the cylindrical structure, which uses the geometry of the structure and only requires simple image processing (line extraction). Then we prove that the proposed observer is globally stable. Preliminary experimental results and simulation results are reasonable and promising, which implies the proposed method has potential to be used in the real AUV navigation applications.**

I. Introduction

Autonomous underwater vehicles (AUVs) have great application potential because working underwater is both dangerous and difficult for humans. Various versions of AUVs have been developed for different applications, such as seabed mapping, underwater structure inspection. Navigation and control are important subtasks in AUV applications. Many control methodologies for underwater robot or underwater vehicle ranging from fuzzy logic control and sliding mode control to adaptive control have been proposed and reported, e.g., [1], [2], [3]. However, vehicle state (orientation, translational position and linear velocity) estimation is an essential prerequisite no matter whether the employed controller belongs to model-based control or model-free control. Although reasonably good state estimation can be achieved through using costly sensors like the Long Baseline, the Ultra-short Baseline, and Doppler Velocity Log ([4], [5], [6]), reliable and accurate AUV state estimation using low cost sensors is still challenging.

In this paper, we consider the problem of state estimation for underwater vehicle that is required to navigate around a cylindrical structure (e.g., for inspection). This vehicle is only equipped with the low-cost sensors: a typical IMU, a pressure sensor and a monocular camera.

Unlike ground mobile robots navigating outdoor, underwater vehicles cannot obtain the required xy coordinates in the horizontal plane via GPS signals because GPS signals are blocked by the water. Hence, the monocular camera becomes a critical resource for localization. In the past decade, the view-based Simultaneous Localization and Mapping (SLAM) approaches have been succeeded in some underwater scenarios ([7], [8]). However, one difficulty of the SLAM problem in the underwater environment is feature extraction and matching, which may require high quality images. Hence, it is desirable to develop a robust and efficient algorithm to localize the underwater vehicle by using the monocular camera without requiring complicated image processing. This could be achieved, for example, by using some prior knowledge about the environment.

On the other hand, the estimation of orientation under the presence of gyroscope bias is another important issue. In [9], three orientation observers formulated in the special orthogonal group $SO(3)$ are proposed, resulting in almost global stability according to Lyapunov stability analysis. In this paper, we follow a similar idea and design a globally stable observer. In addition, we propose to integrate the image information (and the prior knowledge about the environment) with IMU readings for the orientation and gyro bias estimation in order to improve the robustness.

Due to the difficulty of determining the exact dynamics of a complex-shaped underwater robot especially in the open-water environment with varying water current, the empirical plant dynamics (e.g., added mass, nonlinear Coriolis models, hydrodynamic damping forces, etc.) is usually employed as a proxy ([10], [11]). Parameter identification can be done by computational fluid dynamics software ([12], [13]) or practical experiments (e.g., [14]), but in this way only the rough values of plant parameters can be obtained. In addition, the experiment-based parameter identification methods for a complex-shaped underwater robot usually require expensive

devices, such as a towing tank, with dedicated instrumentation and manoeuvres. In this paper, the proposed method does not require the nominal plant dynamics of the underwater vehicle.

Some state estimation approaches employ stochastic estimation methods, such as [15] and [16]. However, there is no general analytical method for propagating non-Gaussian probability distributions for most of nonlinear systems, and most stochastic estimation methods requires linearization (e.g., the extended Kalman filter) or sampling-based method (e.g., particle filter). Therefore, the analytical stability analysis for the stochastic estimation methods is not commonly available [17]. In this paper, we propose a nonlinear state observer, which makes use of the geometry structure of $SO(3)$ and guarantees the global stability when the vehicle's orientation and position are available.

This paper is organized as follows. Section II introduces the notations used and the considered problem. Then a quick overview of the proposed observer is given in Section III. In Section IV, assuming the orientation is known, we firstly present a method to calculate the vehicle's position, which employs the simple image information and the symmetry of the cylinder. Next, we show how to integrate the image information to estimate the vehicle's orientation. In Section V, we prove that our proposed observer is globally stable. In Section VI, preliminary experimental result on localization and simulation results about the proposed observer are reported. Section VII presents the conclusion and future work.

II. Notations and Problem Statement

A. Notations

The special orthogonal group (rotation matrix group) $SO(3)$ is the set, defined as $\{R \in \mathbb{R}^{3\times 3} | \det(R) = 1,\ R^T R = \mathrm{I}_3\}$. The vehicle's orientation can be represented by a rotation matrix. For more details about the special orthogonal group see [18].

The skew symmetric operator s is defined such that $s(x)y = x \times y$ for $x, y \in \mathbb{R}^3$. The operator Υ as the inverse of the operator s is a mapping from 3×3 skew symmetric matrix to 3-dimensional vector, defined as $(s(x))^{\Upsilon} = x$ for $x \in \mathbb{R}^3$.

The operator $\|.\|$ is the Euclidean norm. If v is a vector in the 3-D space, O is a coordinate frame in this 3-D space, then $v|_O$ represents the expression of the vector v in the frame O. Similarly, if c is a point then $c|_O$ represents the coordinates of the point c in the frame O. The symbol $\hat{}$ denotes the estimated value respect to some variable, e.g., if q denotes a variable, then $\hat{q}$ refers to the estimated value of q. The function tr() denotes the trace of a matrix.

B. Problem Statement

Imagine a scenario that an underwater vehicle is navigating around a vertical cylinder with known radius. The vehicle is equipped with a monocular camera, a pressure sensor and a typical IMU (including accelerometer, gyroscope and magnetometer). For simplicity, we consider the condition that the outline of the cylinder can always be seen by the camera. Once a proper calibration for camera is done, one can first undistort the image and then perform line extraction to get the boundary of the cylinder in the image. An example of underwater image taken from the experimental water tank is shown in Fig. 1.

Fig. 1: an underwater image: the cylinder in the experimental water tank

In order to describe the motion of the underwater vehicle, we introduce two coordinate frames: the body frame B fixed in the vehicle and the inertial frame O. The origin of the frame O is chosen in the axis of the cylinder and the Z axis of the inertia frame O is chosen as upward (parallel to the axis of the cylinder). Moreover, the camera's pose relative to the vehicle is fixed and known. For simplicity, it is assumed that the camera frame coincides with the frame B. We denote the state X to be estimated as the form

$$X = (R, b, p, v), \tag{1}$$

where $R \in SO(3)$ as the rotation from the frame B to the frame O denotes the vehicle's orientation in the inertia frame O, $b \in \mathbb{R}^3$ denotes the gyroscope bias, $p \in \mathbb{R}^3$ as the coordinates of the origin B_o of the frame B in the frame O denotes the vehicle's position in the inertia frame O, $v \in \mathbb{R}^3$ denotes the vehicle's linear velocity in the inertial frame O. The differential equation of the state can be expressed as the following

$$\dot{X} = f(X, U), \tag{2}$$

where $U = (\Omega, a)$ and

$$f(X, U) := (Rs(\Omega - b), 0, v, Ra + g), \tag{3}$$

where s is the skew symmetric operator mentioned in Section II-A, $g \in \mathbb{R}^3$ is the known gravitational acceleration expressed in the frame O, $a \in \mathbb{R}^3$ is the proper acceleration that can be measured by the accelerometer and $\Omega \in \mathbb{R}^3$ is the gyroscope reading.

In this paper, we focus on estimating the state (R, b, p, v) by fusing the information from IMU, pressure sensor, image of the cylinder and the prior knowledge of the geometry of the cylinder.

III. The Proposed Observer

In this section, we state the proposed observer under the condition when the vehicle's orientation and position is available (Section IV). In this case, the output of the system (Eq. 2) is

$$Y = h(X) = (R, p). \tag{4}$$

Let $\hat{X} = (\hat{R}, \hat{b}, \hat{p}, \hat{v})$ be the estimated state. Making use of the geometric structure of the special orthogonal group, our proposed observer is designed as

$$\frac{d}{dt}\hat{X} = F(\hat{X}, U, Y), \tag{5}$$

where

$$F(\hat{X}, U, Y) = \begin{pmatrix} \hat{R}s(k_1 \frac{(\hat{R}^T R - R^T \hat{R})^\vee}{\sqrt{1/2 + \mathrm{tr}(\hat{R}^T R)/2}} + \Omega - \hat{b}) \\ -k_2 \Delta\theta \frac{(\hat{R}^T R - R^T \hat{R})^\vee}{\|(\hat{R}^T R - R^T \hat{R})^\vee\|} \\ \hat{v} + 2k_3(p - \hat{p}) \\ Ra + g + k_3(p - \hat{p}) \end{pmatrix}^T, \tag{6}$$

k_i $(i = 1, 2, 3)$ are constant gains, $\Delta\theta \in [0, \pi]$ is the rotation angle of the rotation matrix $\hat{R}R^T$. We can obtain $\Delta\theta$ by the following equation:

$$\Delta\theta = \arccos\left(\frac{\mathrm{tr}(\hat{R}R^T) - 1}{2}\right). \tag{7}$$

In [9], the orientation observers employ the geometric structure of the group $SO(3)$ but they are not globally stable because the error of the estimated orientation and the actual orientation is defined as $1 - \cos\Delta\theta$. Our proposed method also employ the geometric structure of the group $SO(3)$, but takes the orientation error as $\Delta\theta$ for global stability. The theoretical analysis of the observer will be given in Section V.

IV. Localization

Although the proposed observer has been given, how to obtain the observations (R, p) remains an issue. In this section, we will show how to obtain the raw signal of (R, P) by using the information from the sensors and the prior knowledge of the cylinder geometry.

A. Calculate the vehicle's position p if R is known

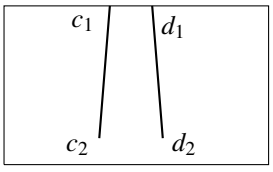

Fig. 2: The projection of the boundary lines of the cylindrical structure on the image plane

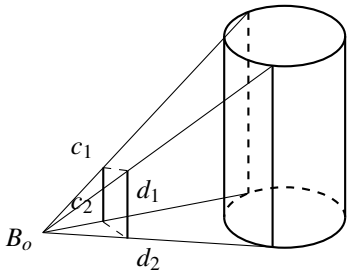

Fig. 3: Projection of the cylinder in the camera/body frame

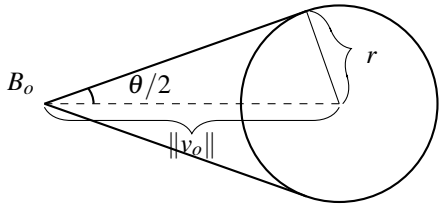

Fig. 4: The top view

In this subsection, it is assumed the vehicle's orientation R is known (how to obtain R will be given in Section IV-B). Because p_z can be easily obtained via the measurement from the pressure sensor, we will only show how to get xy coordinates of the vehicle's position, i.e., (p_x, p_y).

We consider the condition that the outline of the cylinder can always be seen by the camera. Under this condition, the projection of the cylinder on the image plane is two line segments as shown in Fig. 2. We denote one line segment in the image plane as c_1c_2 and the other one as d_1d_2 such that $c_1c_2d_2d_1$ forms a quardrangle. In addition, note that the origin of the camera/body frame B is B_o. Considering the symmetric shape of the cylinder, we have that the line segments c_1c_2 and d_1d_2 must correspond to two straight lines on the surface of the cylinder, which implies that the plane $B_oc_1c_2$ and the plane $B_od_1d_2$ share a common vector that is the direction of the axis of the cylinder. Fig. 3 shows the correspondence. The intrinsic parameters of a well-calibrated monocular camera are known and hence $c_i|_B, d_i|_B \in \mathbb{R}^3$ $(i = 1, 2)$ be obtained.

We define the vector v_o as the vector from the origin B_o of the frame B to the axis of the cylinder (see Fig. 4 and Fig. 5). Let λ be the direction vector of the axis of the cylinder and

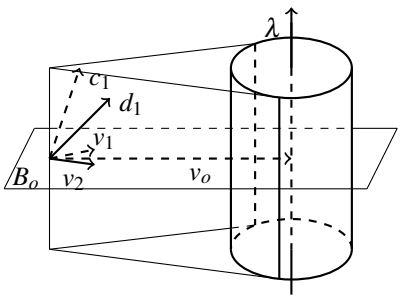

Fig. 5: The vector v_o

$\lambda|_O = [0,0,1]^T$ be the coordinates of λ in the frame O. Note that the plane containing the point B_o, the vector v_o parallels to the xy plane and λ is perpendicular to the xy plane, thus we have

$$v_o|_B = R^T[-p_x, -p_y, 0]^T, \tag{8}$$

where $v_o|_B$ is the expression of the vector v_o in the body frame B. If we have $v_o|_B$, then (p_x, p_y) would be obtained from Eq. 8 because R is assumed to be known. In the following we will show how to calculate $v_o|_B$.

Firstly, we calculate the length $\|v_o\|$ of $v_o|_B$. We can obtain the intersection angle θ between the plane $B_o c_1 c_2$ and the plane $B_o d_1 d_2$:

$$\theta = \arccos \frac{(c_1|_B \times c_2|_B)^T (d_1|_B \times d_2|_B)}{\|c_1|_B \times c_2|_B\| \|d_1|_B \times d_2|_B\|}. \tag{9}$$

Considering that the plane $B_o c_1 c_2$ and the plane $B_o d_1 d_2$ must be tangent to the cylinder and the known radius of the cylinder is r, from Fig. 4 we have

$$\|v_o\| = \frac{r}{\sin(\theta/2)}. \tag{10}$$

Secondly, we show how to calculate the direction vector of $v_o|_B$. Note that the plane $B_o c_1 c_2$ contains the vector λ, hence $\lambda|_B$ as the coordinates of λ in the frame B can be expressed as $k_1 c_1|_B + k_2 c_2|_B$ where k_1 and k_2 are undetermined coefficients. Note that the plane $B_o d_1 d_2$ also contains the vector λ and hence λ is perpendicular to the normal vector of the plane $B_o d_1 d_2$. Therefore, we have

$$(d_1|_B \times d_2|_B)^T (k_1 c_1|_B + k_2 c_2|_B) = 0. \tag{11}$$

On the other hand, λ is a unit vector and hence we have

$$\|(k_1 c_1|_B + k_2 c_2|_B)\| = 1. \tag{12}$$

Eq. 11 and Eq. 12 have two solutions with respect to (k_1, k_2). Actually, there exists an unit vector $m \in \mathbb{R}^3$ such that

$$k_1 c_1|_B + k_2 c_2|_B = \pm m. \tag{13}$$

With the equation $R^T \lambda|_O = \lambda|_B = k_1 c_1|_B + k_2 c_2|_B$, we have

$$R^T \lambda|_O = \pm m. \tag{14}$$

Now we have obtained the expression of $\lambda|_B$, i.e., m or $-m$. Note that v_o is the bisector of angle between the plane $B_o c_1 c_2$ and the plane $B_o d_1 d_2$. Hence v_o is also the bisector of angle of the vector v_1 and the vector v_2, where $v_1 = c_1|_B - (m^T c_1|_B)m$ contained in the plane $B_o c_1 c_2$ is perpendicular to m and $v_2 = d_1|_B - (m^T d_1|_B)m$ contained in the plane $B_o d_1 d_2$ is perpendicular to m as well (Fig. 5). Therefore, we can obtain the direction vector $\frac{v_o|_B}{\|v_o\|}$ of $v_o|_B$ as

$$\frac{v_o|_B}{\|v_o\|} = \mathrm{N}(\mathrm{N}(v_1) + \mathrm{N}(v_2)), \tag{15}$$

where N is the normalization function such that $\mathrm{N}(x) = \frac{x}{\|x\|}$ for $x \in \mathbb{R}^3$.

With Eq. 10 and Eq. 15, we have

$$v_o = \frac{r}{\sin(\theta/2)} \mathrm{N}(\mathrm{N}(v_1) + \mathrm{N}(v_2)). \tag{16}$$

Now we can easily obtain (p_x, p_y) according to Eq. 8.

B. The vehicle's orientation R

The calculation of the vehicle's position p requires the vehicle's orientation R. Denote $s_1^0 \in \mathbb{R}^3$ as the magnetic field in the inertial frame O (a prior knowledge), $s_2^0 \in \mathbb{R}^3$ as the direction vector of the gravitational vector expressed in the inertia frame O (a prior knowledge), and $s_1 \in \mathbb{R}^3$ as the direction vector of the measurement from the magnetometer and $s_2 \in \mathbb{R}^3$ as the negative direction vector of the measurement from the accelerometer. Similar to the method in [9], the vehicle's orientation R can be roughly estimated by

$$R = \underset{R_y \in SO(3)}{\operatorname{argmin}} \Sigma_{i=1}^2 \|R_y s_i - s_i^0\|^2 + \|R_y m - \mathrm{sgn}(m^T s_2)\lambda|_O\|^2. \tag{17}$$

Unlike most nonlinear optimization problems, the nonlinear optimization problem Eq. 17 has an efficient and unique solution [19].

So far, we have explained how to get the vehicle's pose (R, p) by using the sensors and the prior knowledge.

V. The Analysis of the Proposed Observer

In this section, we prove that the proposed observer is globally stable.

For simplifying the stability analysis, we define two Lyapunov functions V_1 and V_2 as the following:

$$V_1 = \frac{1}{2}\Delta\theta^2 + \frac{1}{2k_2}\|\hat{b} - b\|^2, \tag{18}$$

$$V_2 = \begin{pmatrix} p - \hat{p} \\ v - \hat{v} \end{pmatrix}^T P \begin{pmatrix} p - \hat{p} \\ v - \hat{v} \end{pmatrix}^T, \tag{19}$$

where $P = \begin{pmatrix} \frac{k_3+1}{2k_3}\mathbf{I}_3 & \mathbf{I}_3 \\ \mathbf{I}_3 & \frac{5k_3+1}{2}\mathbf{I}_3 \end{pmatrix}$ is a positive definite matrix for $k_3 > 0$. Note that we have the following equation about the rotation angle $\Delta\theta$

$$2\sin\Delta\theta = \|(\hat{R}^T R - R^T \hat{R})^\vee\|. \tag{20}$$

With Eq. 3 (the first two terms), Eq. 6 (the first two terms), Eq. 7, Eq. 18 and Eq. 20, after some tedious but simple calculation, we have

$$\begin{aligned}
\dot{V}_1 &= \frac{d}{dt}(\frac{1}{2}\Delta\theta^2 + \frac{1}{2k_2}\|b - \hat{b}\|^2) \\
&= \Delta\theta\Delta\dot{\theta} + \frac{1}{k_2}(\hat{b} - b)^T \dot{\hat{b}} \\
&= \Delta\theta(-\frac{2k_1 \sin\Delta\theta}{\sqrt{1+\cos\Delta\theta}} - W_r^T(\hat{b} - b)) \\
&\quad - (\hat{b} - b)^T \frac{\Delta\theta(\hat{R}^T R - R^T \hat{R})^\vee}{\|(\hat{R}^T R - R^T \hat{R})^\vee\|} \\
&= -\frac{2k_1\Delta\theta\sin\Delta\theta}{\sqrt{1+\cos\Delta\theta}} - \Delta\theta W_r^T(\hat{b} - b) + (\hat{b} - b)^T \Delta\theta W_r \\
&= -\frac{2k_1\Delta\theta\sin\Delta\theta}{\sqrt{1+\cos\Delta\theta}} \leq -\frac{2\sqrt{2}}{\pi}k_1\Delta\theta^2
\end{aligned} \tag{21}$$

for $\Delta\theta \in [0, \pi]$, where $W_r = \frac{-(\hat{R}^T R - R^T \hat{R})^\vee}{\|(\hat{R}^T R - R^T \hat{R})^\vee\|} \in \mathbb{R}^3$ is the rotation axis of $R^T \hat{R}$. Hence it is followed that $\Delta\theta \to 0$, i.e., $\hat{R} \to R$.

Then we can prove $\hat{b} \to b$. Note that $\hat{R} \to R$ implies $\dot{\hat{R}} \to \dot{R}$. With Eq. 3 (the first term) and Eq. 6 (the first term), $\hat{R} \to R$ and $\dot{\hat{R}} \to \dot{R}$ imply $\hat{b} \to b$.

On the other hand, with Eq. 2 (the last two terms), Eq. 6 (the last two terms) and Eq. 19, we have

$$\begin{aligned} \dot{V}_2 &= \frac{d}{dt}\begin{pmatrix} p-\hat{p} \\ v-\hat{v} \end{pmatrix}^T P \begin{pmatrix} p-\hat{p} \\ v-\hat{v} \end{pmatrix} \\ &= \begin{pmatrix} p-\hat{p} \\ v-\hat{v} \end{pmatrix} (A_c P + P A_c^T) \begin{pmatrix} p-\hat{p} \\ v-\hat{v} \end{pmatrix}, \\ &= -2k_3(\|p-\hat{p}\|^2 + \|v-\hat{v}\|^2) \leq 0 \end{aligned} \tag{22}$$

where

$$A_c = \begin{pmatrix} -2k_3\mathbf{I}_3 & \mathbf{I}_3 \\ -k_3\mathbf{I}_3 & 0_{3\times 3} \end{pmatrix}. \tag{23}$$

Eq. 22 results in $\hat{p} \to p$ and $\hat{v} \to v$. In all, $\hat{X} \to X$, i.e., the estimated state converges to the actual state.

VI. Experiment and Simulation Results

Now we present some results using the proposed methods. In Section VI-A, preliminary results of experiment about localization are presented, which verifies the method in Section IV to some extent. In Section VI-B, numerical simulations have been performed in order to show the effectiveness and robustness of the proposed observer in Section III.

A. The Preliminary Results of Experiment about Localization

The underwater vehicle in our lab requires a bit more instrumentation before we can perform the full testing. In order to test the proposed localization method, some underwater images from different locations were taken by the camera Genius KYE F100 with waterproof enclosure in our water tank where there is a vertical cylinder with $0.3m$ radius. The resolution of the images is 1280×720. One example image is shown in Fig. 1. For every shot, we manually measured the roll and pitch of the camera and the distance between the camera and the cylinder.

For each image, we extracted line segments c_1c_2 and d_1d_2 and calculated $\|v_o\| \in \mathbb{R}^+$ (Eq. 10) and $m \in \mathbb{R}^3$ (Eq.13). Note that $\|v_o\|$ refers to the distance from the camera to the axis of the cylinder, m is the vertical upward vector expressed in the camera frame. Next, we calculated the roll θ_r and pitch θ_p of the camera by using Eq. 14 and m. Then we compared $\|v_o\|$, θ_r and θ_p with the corresponding measurements.

Some example results are listed in Table I in which the superscript M denotes the measured value. It is shown in Table I that the calculation results by the method in Section IV are very close to the measurements with error less than 4% for $\|v_o\|$ and less than 7% for the angles. The experiment results validates the proposed method for localization to some extent.

	$\|v_o\|$	$\|v_o\|^M$	θ_r	θ_r^M	θ_p	θ_p^M
1	3.72m	3.75m	77.8°	≈ 80°	83.0°	≈ 85°
2	3.42m	3.52m	168.5°	≈ 175°	80.0°	≈ 85°
3	3.93m	3.87m	153.0°	≈ 160°	81.0°	≈ 85°
4	3.79m	3.82m	140.3°	≈ 145°	88.3°	≈ 85°
5	3.37m	3.33m	179.2°	≈ 180°	82.5°	≈ 85°

TABLE I: calculation results vs measurements

B. Simulation Results of the Proposed Observer

In this subsection, we perform the numerical simulations to validate our proposed observer (Eq. 6) under the condition (R, p) is available. In the following, all units of the values are the international units. For generating ground truth, we simulate a virtual underwater vehicle navigating around a cylindrical structure. The simulated trajectory is helical designed as the following: $R(t) = \exp\{s((0,0,1)^T)\pi t/10\}$ and $p(t) = [-5\cos(\pi t/10), -5\sin(\pi t/10), t/20]^T$ (unit: m). The actual rate gyro bias is set as $[0.5, -0.5, 0.3]^T$ (unit: rad/s). The initial state estimation value $(\hat{R}, \hat{b}, \hat{p}, \hat{v})$ is set as $\hat{R}(0) = \mathrm{I}_3$, $\hat{b}(0) = [0,0,0]^T$ (unit: rad/s), $\hat{p}(0) = [-5,0,0]^T$ (unit: m), and $\hat{v}(0) = [0,0,0]^T$ (unit: m/s).

For verifying the robustness of the proposed observer, the noises are added into the observations (R, p) and the IMU readings (Ω, a). The raw orientation is set as $\exp(\frac{5\pi\sin(t)}{180} s(q(t)))R(t)$, where $q(t) \in \mathbb{R}^3$ is a time-vary random unit vector. This setting would lead to the average 3.2 degree error of orientation. The gyro readings is added with a Gaussian white noise vector whose standard deviation is $[0.05, 0.05, 0.05]^T$ (unit: rad/s). The raw position measurement is added with a Gaussian white noise vector whose standard deviation is $[0.05, 0.05, 0.05]^T$ (unit: m). The proper acceleration is added with a Gaussian white noise vector whose standard deviation is $[0.05, 0.05, 0.05]^T$ (unit: m/s^2). The gravitational acceleration g is set as $[0, 0, -9.81]$ (unit: m/s^2). Note that the performance of the nonlinear filter is largely dependent on the parameters. Hence, we carefully tune the parameters as follows: $k_1 = 1$, $k_2 = 1$, $k_3 = \sqrt{2}$. In addition, all available measurements' frequency is set as 20 Hz.

To show the simulation results more effectively, we present the results of the estimated orientation and position in TABLE II where AVE refers to the average error after convergence and OAVE refers to the average error of the observations (R, p). The error of the estimated orientation is the rotation angle $\Delta\theta$ of $R^T\hat{R}$ (Eq. 7) while the error of the estimated position $\hat{p}$ is $\|p - \hat{p}\|$. In TABLE II, we can see the estimated orientation and the estimated position from the proposed observer have better precision than the raw observations (R, p).

	AVE	OAVE
orientation	2.5°	3.32°
x-position	$0.018m$	0.025m
y-position	$0.017m$	0.025m
z-position	$0.016m$	0.025m

TABLE II: The estimated orientation and position

The history of the estimated gyroscope bias $\hat{b} = (b_1, b_2, b_3)^T$ is displayed in Fig. 6. At the beginning, the initial estimated bias is $[0,0,0]^T$, far away from the actual value $[0.5, -0.5, 0.3]^T$. The "actual bias" is set as much bigger than the normal value but the proposed observer can still estimate the bias accurately after 6 seconds.

The error $\Delta v = (\Delta v_1, \Delta v_2, \Delta v_3)^T$ of the estimated velocity refers to $\hat{v} - v$, which is shown in Fig. 7. We can see that the estimated velocity $\hat{v}$ along the y axis converges to the actual velocity very quickly (after 6 seconds) although the initial error is set to be very large. The proposed observer with respect to the velocity also performs well.

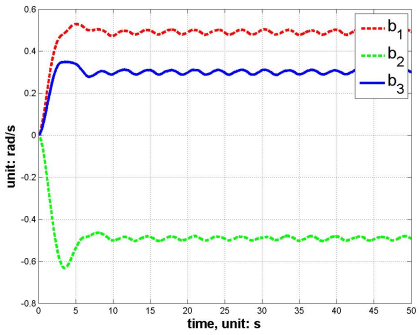

Fig. 6: The estimation of gyroscope bias

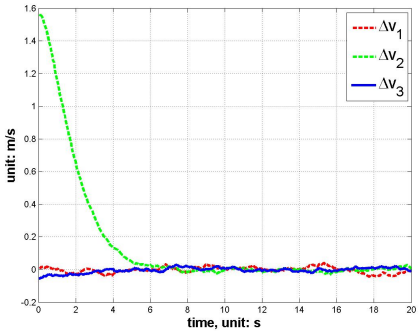

Fig. 7: The error of estimated velocity

VII. Conclusion and Future Work

We have considered the problem of state estimation for underwater vehicle navigation around a cylindrical structure. Under some reasonable assumptions, we firstly present a method to localize the vehicle via the low-cost on-board sensors and some prior knowledge about the environment, which makes use of the symmetric property of the cylinder. The way to integrate the image information into the orientation estimation is also discussed. Secondly, we propose an observer that ensures the global stability according to two Lyapunov functions. The preliminary results of experiment and simulation are promising and validate our proposed method. For the future work, more experiments will be performed for further validating and improving. We may also modify the method to accommodate various scenarios such as a rectangular-shaped structure.

Acknowledgment

This work is supported in part by the Joint Centre for Robotics Research (JCRR) between the University of Technology, Sydney and Zhejiang University. The authors are all with the JCRR.

References

[1] G. Antonelli and A. Leonessa, "Underwater robots: Motion and force control of vehicle-manipulator systems," *IEEE Control Systems Magazine*, 2008.

[2] L. Whitcomb and D. Yoerger, "Preliminary experiments in model-based thruster control for underwater vehicle positioning," *Oceanic Engineering, IEEE Journal of*, vol. 24, no. 4, pp. 495–506, 1999.

[3] S. Zhao and J. Yuh, "Experimental study on advanced underwater robot control," *Robotics, IEEE Transactions on*, vol. 21, no. 4, pp. 695–703, 2005.

[4] A. Alcocer, P. Oliveira, and A. Pascoal, "Study and implementation of an {EKF} gib-based underwater positioning system," *Control Engineering Practice*, vol. 15, no. 6, pp. 689 – 701, 2007, special Section on Control Applications in Marine Systems CAMS2004 Control Applications in Marine Systems.

[5] B. Jalving, K. Gade, O. Hagen, and K. Vestgard, "A toolbox of aiding techniques for the hugin auv integrated inertial navigation system," in *OCEANS 2003. Proceedings*, vol. 2, Sept 2003, pp. 1146–1153 Vol.2.

[6] R. McEwen, H. Thomas, D. Weber, and F. Psota, "Performance of an auv navigation system at arctic latitudes," *Oceanic Engineering, IEEE Journal of*, vol. 30, no. 2, pp. 443–454, April 2005.

[7] C. Roman and H. Singh, "A self-consistent bathymetric mapping algorithm," *Journal of Field Robotics*, vol. 24, no. 1-2, pp. 23–50, 2007.

[8] R. Garcia, J. Batlle, X. Cufi, and J. Amat, "Positioning an underwater vehicle through image mosaicking," in *Robotics and Automation, 2001. Proceedings 2001 ICRA. IEEE International Conference on*, vol. 3, 2001, pp. 2779–2784 vol.3.

[9] R. Mahony, T. Hamel, and J. Pflimlin, "Nonlinear complementary filters on the special orthogonal group," *Automatic Control, IEEE Transactions on*, vol. 53, no. 5, pp. 1203–1218, June 2008.

[10] J. Kinsey and L. Whitcomb, "Model-based nonlinear observers for underwater vehicle navigation: Theory and preliminary experiments," in *Robotics and Automation, 2007 IEEE International Conference on*, April 2007, pp. 4251–4256.

[11] C. McFarland and L. Whitcomb, "Experimental evaluation of adaptive model-based control for underwater vehicles in the presence of unmodeled actuator dynamics," in *Robotics and Automation (ICRA), 2014 IEEE International Conference on*, May 2014, pp. 2893–2900.

[12] R. Yang, B. Clement, A. Mansour, M. Li, and N. Wu, "Modeling of a complex-shaped underwater vehicle for robust control scheme," *Journal of Intelligent & Robotic Systems*, pp. 1–16, 2015.

[13] M. Hosny, M. Amr, I. Zedan, M. AbdelSalam, and M. Al-Sayd, "Computational fluid dynamics-based system identification of marine vehicles," in *Computing, Communication and Networking Technologies (ICCCNT), 2014 International Conference on*, July 2014, pp. 1–7.

[14] D. Smallwood and L. Whitcomb, "Preliminary experiments in the adaptive identification of dynamically positioned underwater robotic vehicles," in *Intelligent Robots and Systems, 2001. Proceedings. 2001 IEEE/RSJ International Conference on*, vol. 4, 2001, pp. 1803–1810 vol.4.

[15] E. J. Lefferts, F. L. Markley, and M. D. Shuster, "Kalman filtering for spacecraft attitude estimation," *Journal of Guidance, Control, and Dynamics*, vol. 5, no. 5, pp. 417–429, 1982.

[16] B. Barshan and H. F. Durrant-Whyte, "Inertial navigation systems for mobile robots," *Robotics and Automation, IEEE Transactions on*, vol. 11, no. 3, pp. 328–342, 1995.

[17] A. Barrau and S. Bonnabel, "The invariant extended kalman filter as a stable observer," *CoRR*, vol. abs/1410.1465, 2014. [Online]. Available: http://arxiv.org/abs/1410.1465

[18] R. M. Murray, Z. Li, S. S. Sastry, and S. S. Sastry, *A Mathematical Introduction To Robotic Manipulation*. CRC press, 1994.

[19] S. Umeyama, "Least-squares estimation of transformation parameters between two point patterns," *Pattern Analysis and Machine Intelligence, IEEE Transactions on*, vol. 13, no. 4, pp. 376–380, Apr 1991.